

## Two-magnon processes and ferrimagnetic linewidth calculation in manganese ferrite

A. G. Flores,\* V. Raposo, L. Torres, and J. Ñíguez

*Departamento de Física Aplicada, Universidad de Salamanca, E-37071 Salamanca, Spain*

(Received 2 June 1998; revised manuscript received 28 October 1998)

A procedure has been developed to obtain the two-magnon linewidth contributions in single and polycrystalline ferrites in which, working with ferrimagnetic resonance experiments, the applied field was only slightly larger than the value required to saturate the sample. This theory has been shown to work in manganese ferrites. Single-crystal  $\text{MnFe}_2\text{O}_4$  has been prepared by the floating-zone technique and polycrystalline ferrite by the ceramic method. The spinel structure and composition have been confirmed by x-ray and inductively coupled plasma spectrometry, respectively. Fitting of the experimental ferrimagnetic resonance linewidth obtained by means of the Bloch-Bloembergen formalism show errors less than 4%. The fit gave the following parameters: averaged radius of the sample surface pits, porosity in polycrystalline sample, activation energy, and values of the conductivity. The values of the activation energy imply the existence of  $\text{Fe}^{2+}$  cations in the sample. Additional measurements on magnetization in manganese ferrites are presented.

[S0163-1829(99)00214-3]

### I. INTRODUCTION

The magnetic properties of manganese ferrites have been a subject of interest in the last few years. The general question of what happens to the bulk properties of a macroscopic body as one or more of its dimensions are reduced to atomic size,<sup>1,2</sup> the behavior of the size-dependent Curie temperature,<sup>1-5</sup> the study of the variation of the magnetization with temperature,<sup>1</sup> the cation distribution,<sup>6</sup> and the ferrimagnetic resonance linewidth due to scattering of the uniform magnon have been some of the main studies.<sup>7,8</sup>

The selection of manganese for this work was based on the importance of this cation in different kinds of materials. The recently rediscovered "colossal magnetoresistance" in the perovskite manganate  $R_{1-x}B_x\text{MnO}_3$  (with  $R=\text{La, Pr, Nd, Sm}$  and  $B=\text{Ca, Sr, Ba, Pb}$ ) has renewed attention in these systems.<sup>9-13</sup> The difficulty one faces when studying these systems is to make sure that the samples are well characterized and of good quality. Compounds prepared under similar conditions often exhibit different properties.<sup>14</sup> X-ray powder diffraction frequently does not indicate the presence of spurious phases or any evidence that would suggest that the samples are inhomogeneous. On the other hand, it has been shown that magnetic resonance is an extremely sensitive and useful technique to study the quality of the samples in these systems.<sup>15,16</sup>

Because of these reasons and the ample experience of our group in ferrimagnetic resonance (FMR),<sup>17-24</sup> the goal of this work is to study the FMR linewidth in single and polycrystalline manganese ferrite. In particular, we developed a two-magnon linewidth calculation for these ferrites which do not support Sparks' and Schlömann's theories.<sup>25,26</sup>

### II. THEORY

The microscopic theory of the two-magnon process is based on a simple model in which one magnon of the uniform precession is annihilated and another magnon with the same energy and nonzero wave vector called "degenerate

magnon" is created. The scattering from the uniform precession to the degenerate mode is an important relaxation source in magnetic materials, such as spinel ferrites, and can be induced by different mechanisms: pits left on the surface of the sample by the polishing process, pores between the grains in polycrystalline samples, random orientation of the anisotropy energy axes from grain to grain, etc.

A physical description of the two-magnon linewidth process has been fully investigated by different authors.<sup>25-30</sup> Sparks has calculated the two-magnon linewidth induced by pits left on the surface of isotropic spherical samples.<sup>27</sup> In this approach, a surface pit is represented by a single spherical void in an infinite medium. This void will produce a demagnetization field with its axis along the magnetization direction. If the magnetization precess (for example, the uniform precession), the demagnetization field will be modulated at the precession frequency. The interaction between the modulated demagnetization field and a degenerate magnon will change the energy of both the uniform precession and the degenerate magnon. The main results obtained from this highly oversimplified model are physically reasonable.

The analysis to determine the two-magnon contribution to the FMR linewidth is based on the transition probability calculation. This requires the dispersion relation to be calculated and the Hamiltonian to be diagonalized by means of Holstein-Primakoff transformations.<sup>27</sup> Making the first and the second transformation it is possible to approximate the Hamiltonian into the diagonal form. In this case the dispersion relation obtained is

$$\hbar \omega_k = Dk^2 + \hbar \omega_i + (1/2)\hbar \omega_m \sin^2 \theta_k, \quad (1)$$

where  $\omega_i = \gamma H_i = \gamma(H_0 - 4\pi N_z M)$  ( $\gamma$  is the absolute value of the electron gyromagnetic ratio,  $H_0$  is the resonance field,  $N_z$  is the  $z$  component of the demagnetizing tensor, and  $M$  is the dynamic magnetization),  $\omega_m = 4\pi\gamma M_S$ ,  $\omega_u = \gamma H_0 = \omega_0$  ( $\omega_u$  is the frequency of the uniform mode at resonance. For spherical samples,  $\omega_u = \omega_0$ ),<sup>27</sup> the  $D$  parameter characterizes

the strength of the exchange and  $\theta_k$  is the angle between the wave vector  $k$  and the internal static field  $H_i$ .

If the third Holstein-Primakoff transformation is made,<sup>27</sup> the exact dispersion relation is found:

$$\hbar \omega_k = [(Dk^2 + \hbar \omega_i)(Dk^2 + \hbar \omega_i + \hbar \omega_m \sin^2 \theta_k)]^{1/2}. \quad (2)$$

The set of curves for all values of  $\sin^2 \theta_k$  is called the *spin-wave manifold* (SWM). The complete spectrum for  $k=0$  lies in a frequency band between  $\gamma H_i$  and  $\gamma[H_i(H_i + 4\pi M_S)]^{1/2}$ .

This two-magnon analysis has been limited to materials which are either isotropic or have relatively small levels of magnetocrystalline anisotropy so that the behavior of the spin-wave band is essentially the same as for isotropic materials. Schlömann,<sup>26</sup> among others, has shown that anisotropy can have a significant effect on the spin-wave dispersion and the corresponding SWM. The effect of anisotropy has been fully developed in anisotropic ferrite films by Hurben.<sup>30</sup> The objective of this work, as is related above, is to develop a two-magnon linewidth calculation in manganese ferrite which is an isotropic material, and so Sparks' theory will be valid for now.

In most cases of practical interest the dispersion relation used is the one given by Eq. (1), simplifying, in a great manner, the calculus. The expression obtained for the linewidth is then<sup>27</sup>

$$\Delta H_{\text{sup}} = 4\pi M_S \frac{R}{r_0} \frac{\pi^2}{128} \frac{\omega}{\omega_i} \frac{[(3 \cos^2 \theta_u - 1)^2 + 1.6]}{\cos \theta_u}, \quad (3)$$

where  $R$  is the pit radius,  $r_0$  is the sample radius, and  $\theta_u$  is the angle between the wave vector  $k$  of a magnon in the limit as  $k$  approaches zero (the uniform magnon) and the static field.

However, the approximation of Eq. (1) is very good except for the case in which at least one of the following conditions is fulfilled:<sup>27</sup> (1)  $k$  is very small, (2)  $\sin^2 \theta_k$  is not small, and (3) the applied field is only slightly larger than the value  $4\pi N_z M_S$  required to saturate the sample. In any of these three cases the third Holstein-Primakoff transformation is necessary.

The first case,  $k$  very small, has been studied in spherical samples by Walker.<sup>31</sup> In a classical ferromagnetic resonance experiment a spheroid is placed with its symmetry axis along a uniform static magnetic field strong enough for saturation; if a uniform rf magnetic field is applied in the perpendicular direction across the sample, the dipoles precess in phase together about the demagnetized internal static magnetic field. This will give rise to a single, symmetrical peak in the absorbed power as a function of static field at resonance. However, when the sample is not small enough or when it is placed at a point in the cavity where the rf magnetic field is sufficiently inhomogeneous to vary even over the small sample, a much more complicated absorption curve is observed with a large number of peaks whose position is independent of the frequency and the applied field.<sup>31-34</sup> These peaks have been classified by Walker as the magnetostatic modes. They are important for low values of  $k$ , so the uniform mode of precession ( $k=0$ ) can be considered as a spe-

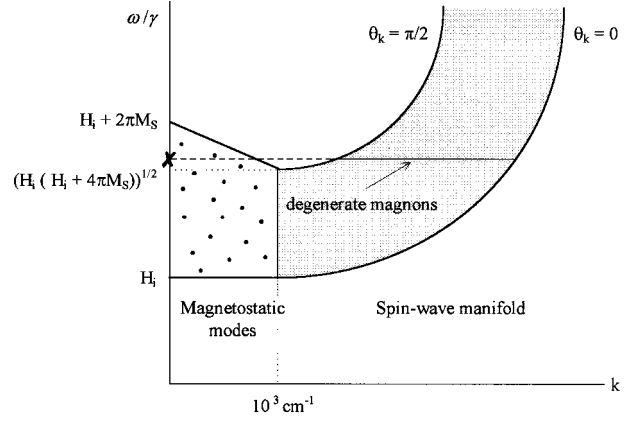


FIG. 1. Relation dispersion spectrum and position of the uniform precession mode ( $\times$ ).

cial instance of such a magnetostatic mode. The complete magnetostatic spectrum lies in a frequency band between  $\gamma H_i$  and  $\gamma(H_i + 2\pi M_S)$ .

The second and the third cases,  $\sin^2 \theta_k$  not small and the applied field only slightly larger than the value required to saturate the sample, respectively, have not been analyzed. No expression is given to obtain the FMR linewidth because of the complexity of substituting the third Holstein-Primakoff in Eq. (2).

We are going to report an experimental procedure to obtain this linewidth in cases in which the ferromagnetic resonance frequency is such that the applied field saturates the sample and the resonance frequency is out of the SWM but inside the magnetostatic spectrum. This situation is shown in Fig. 1.

In this case, (frequency out of the SWM) but with a single and symmetrical peak in the absorption curve, Sparks' theory is not valid to explain the scattering of the uniform mode. We propose a model in which this uniform mode of precession relaxes first to other magnetostatic modes with the same frequency and after that with the different modes of the spin-wave manifold as it can be seen in Fig. 1.

It is to be noted that the modes dominating the relaxation induced by pits on the surface are those with wavelength ( $\lambda = 2\pi/k$ ) which is on the same order of magnitude as the pit radius.<sup>27,28</sup> The radius of the pits in these samples are around  $50 \mu\text{m}$  which implies  $k \approx 1.3 \times 10^3 \text{ cm}^{-1}$ . Looking at Fig. 1, this case corresponds to a mode in the spin-wave manifold, close to  $\theta = \pi/2$ . However, all modes are taken into account. Since the procedure that has been followed to obtain the linewidth is the same as the one proposed by Sparks, the relaxation time for the uniform mode has been obtained by integrating from  $k=0$  to  $k=k_{\text{max}}$  (the maximum wave vector of a magnon degenerate with the uniform precession).<sup>27</sup>

As the dominating contribution is the one given by the mode with  $\theta = \pi/2$ , if we substitute this angle into Eq. (3), the superficial ferrimagnetic resonance linewidth given by Sparks goes to infinity. Taking into account that the relation between  $\theta_u$  and the static field  $H_0$  is given by

$$\cos^2 \theta_u = \frac{H_0 - (2/3)4\pi M_S}{3[H_0 - (1/3)4\pi M_S]}, \quad (4)$$

and that for spherical samples  $\omega_i = \gamma H_i = \gamma [H_0 - (4/3)\pi M]$ ,  $\omega_u = \gamma H_0 = \omega_0$ , we can rewrite Eq. (3) in the following form:

$$\Delta H_{\text{sup}} = 4\pi M_S \frac{R}{r_0} \frac{\pi^2}{128} \frac{3H_0}{3H_0 - 4\pi M_S} \times \left[ \left( \frac{4\pi M_S}{3H_0 - 4\pi M_S} \right)^2 + 1.6 \right] G(\theta_u) \quad (5)$$

with  $G(\theta_u) = 1/\cos \theta_u$ .

If we substitute  $\theta_u = \pi/2$  in this equation, the only part which diverges is the function  $G(\theta_u)$ . We propose to use this expression to calculate the linewidth of the superficial contribution, assuming  $G(\theta_u)$  does not change with temperature and calculating  $G(\theta_u)$  through experimental results from single-crystal experimental data.

In polycrystalline samples there are additional sources of two-magnon linewidths.<sup>27,35,36</sup> Considering first the effect of the pores between the grains, Sparks proposes the following contribution to the linewidth by a similar treatment given in superficial contribution.<sup>27</sup>

$$\Delta H_{\text{por}} = \frac{\pi}{8} 4\pi M_S \frac{V_{\text{pits}}}{V} \frac{\omega}{\omega_i} \frac{[(3 \cos^2 \theta_u - 1)^2 + 1.6]}{\cos \theta_u}, \quad (6)$$

where  $V$  is the sample volume and  $V_{\text{pits}}/V$  is the fraction of the sample occupied by pores, frequently called porosity ( $p$ ). This contribution is by the pores inside the sample, responsible for an additional demagnetization term to the Hamiltonian. Depending on the technique used in the fabrication of the sample this value varies between 3 and 5%.

This expression, equivalent to the one given by the superficial contribution, is valid for frequencies situated inside the SWM spectrum. Following the same treatment as we used before, Eq. (6) can be written as

$$\Delta H_{\text{por}} = \frac{\pi}{8} 4\pi M_S p \frac{3H_0}{3H_0 - 4\pi M_S} \times \left[ \left( \frac{4\pi M_S}{3H_0 - 4\pi M_S} \right)^2 + 1.6 \right] G(\theta_u), \quad (7)$$

where  $p$  is the porosity of the sample (defined above as  $p = V_{\text{pits}}/V$ ) and  $G(\theta_u) = 1/\cos \theta_u$ . The value of  $G(\theta_u)$  is the same obtained for the superficial contribution. This value has been calculated for the single crystal and the same value will be used for the porosity contribution in polycrystalline samples.

Another important source of losses in polycrystalline samples is the random orientation of the anisotropy energy axes from grain to grain. The contribution from this source to the FMR linewidth was studied by Schlömann.<sup>26,37</sup> In polycrystalline ferrites with large anisotropy ( $H_A \gg 4\pi M_S$ ), the dipolar interaction can be neglected when it is compared to anisotropy inside each grain. In this case, the individual grains go through resonance independently at a frequency and at a resonance field determined by the anisotropy field and the orientation of each grain. The shape of the resonance line is essentially determined by the number of grains that go through resonance in a given range of the applied static field.

As long as the anisotropy field is decreased with respect to  $4\pi M_S$  this independent-grain approach loses validity, dipolar interaction dominates and grains resonate all together (for example in the uniform mode). Now, the fluctuation of orientation of the anisotropy energy axes from grain to grain can be considered to be a perturbation. Consequently, the additional term to the Hamiltonian is given by this fluctuation of the anisotropy. The contribution to the linewidth given by Schlömann for a spherical sample is

$$\Delta H_a = \frac{8\pi\sqrt{3}}{21} \frac{H_a^2}{4\pi M_S} \left[ \frac{\Omega^2 - \Omega/3 + 19/360}{\sqrt{(\Omega - 1/3)^3(\Omega - 2/3)}} \right], \quad (8)$$

where

$$\Omega = \frac{\omega}{\gamma 4\pi M_S} = \frac{H_0}{4\pi M_S}; \quad H_a = \frac{-4(3K_1 + K_2)}{9M_S}, \quad (9)$$

and  $K_1$  and  $K_2$  are the first and second anisotropy constant, respectively.

The treatment followed by Schlömann, the same as the one applied by Sparks, is only valid if the operational frequency is inside the SWM. Doing the same suppositions in superficial and porosity contributions, and using the relationship between fields and  $\cos \theta_u$ , Eq. (8) can be written in the following form:

$$\Delta H_a = \frac{\pi}{105} \frac{H_a^2}{4\pi M_S} \left[ \frac{360 - 120\alpha + 19\alpha^2}{(3 - \alpha)^2} \right] G(\theta_u) \quad (10)$$

with  $\alpha = 4\pi M_S/H_0$  and  $G(\theta_u)$  is the same as in the superficial contribution.

As we will demonstrate in the next section, in situations where the frequency of the homogeneous mode lies above the spin-wave spectrum, but inside the range of frequencies of magnetostatic modes, a very small anisotropy broadening is predicted. Because of that we are able to say that the most important sources of relaxation in two-magnon scattering are the superficial and porosity contributions.

Apart from two-magnon scattering there exist other sources of relaxation in single and polycrystals. Because they are not the purpose of this paper we are only going to present them as follows.

*Three mechanisms which give rise to a linewidth showing a maximum as a function of temperature:*

(i) *Valence-exchange mechanism.* It is important in high-conductivity spinel ferrites. This contribution is a possible source of linewidth in crystals containing both  $\text{Fe}^{2+}$  and  $\text{Fe}^{3+}$  ions on equivalent sites in a crystal.

(ii) *Presence of a slowly relaxing impurity.* In this situation, a paramagnetic ion plays a role quite similar to that of the extra  $3d$  electron in the valence-exchange mechanism.

(iii) *Rapidly relaxing impurity.* Just as in the slowly-relaxing-impurity case the  $\text{Fe}^{3+}$  is indirectly coupled by the exchange coupling with the rare-earth impurity, however, the relaxation time is very small.

*Kasuya-Le Craw.* It is the confluence of a uniform-precession magnon with a phonon to form a second magnon. It is a uniform precession to the lattice relaxation process. This mechanism is dependent on frequency, temperature, and the magnetization.

*Eddy-current-loss.* It is important at high temperatures according to a semiconductor behavior. It involves a loss of energy from the uniform precession to the lattice through the conduction electrons without involving the degenerate or thermal magnons. In the cases in which the skin depth is large with respect to the sample size, eddy-current-loss is dependent on sample size, conductivity, and frequency.

In the samples presented below, apart from two-magnon mechanism, eddy-current contribution is also present. In  $\text{MnFe}_2\text{O}_4$ , the skin depth can be considered large with respect to the 0.4 mm spherical radius of the sample and so the eddy-current contribution to the linewidth is given by<sup>27</sup>

$$\Delta H_{ed} \approx \frac{2\pi^2}{c^2\gamma} \sigma r_0^2 \omega^2, \quad (11)$$

where  $r_0$  is the radius sample,  $c$  is the speed of light, and  $\sigma$  is the conductivity given by<sup>39</sup>

$$\sigma = \frac{C}{T} \exp\left(-\frac{E}{kT}\right) \quad (12)$$

with  $C$  a constant independent of temperature,  $E$  is the activation energy of the process, and  $k$  is Boltzmann's constant.

### III. RESULTS AND DISCUSSION

In this section we present the analysis of the two-magnon linewidth in single and polycrystalline manganese ferrite,  $\text{Mn}_{1.0}\text{Fe}_{2.0}\text{O}_4$ . The single crystal was grown by the floating-zone technique and annealed for 72 h in  $\text{CO}_2$  at temperatures between 1150 and 1190 °C. The polycrystalline sample was fabricated by the ceramic method in a thermogravimetric equipment manufactured by Setaram, model no: TG-DTA 92. The sample was sintered at 1300 °C for 4 h in  $\text{CO}_2$  atmosphere. Both samples were characterized by x-ray diffraction, while inductively coupled plasma spectrometry showed a nominal composition.

In order to carry out FMR measurements, the samples were fabricated into spheres with diameters between 0.7 and 0.8 mm. FMR experiments were accomplished by monitoring the reflected wave in a  $\text{TE}_{111}$  mode cylindrical cavity working at X band frequency (8.9 GHz). A dielectric support (teflon) with a center hole was placed at the bottom of the cavity to introduce the sample in such way that it was free to orientate along the external field. The system is fully computerized and the operational temperature range is 77–320 K. At each temperature the full FMR line shape was stored in order to analyze the real and imaginary part of the susceptibility and obtain the FMR linewidth by means of a nonlinear fitting technique: a modified version of the torque equation involving the addition of phenomenological damping terms which account for the relaxation of the magnetization being used. In this work the Bloch-Bloembergen formalism is used because it is physically consistent with the two-magnon processes. The relationship between the imaginary part of the susceptibility and FMR linewidth and resonance field is given by

$$\frac{\chi''}{\chi''_{\max}} = \frac{(\Delta H/2)^2 H [4H_0^2 + (\Delta H/2)^2]}{H_0 [(H_0^2 - H^2 + (\Delta H/2)^2)^2 + 4H^2 (\Delta H/2)^2]}, \quad (13)$$

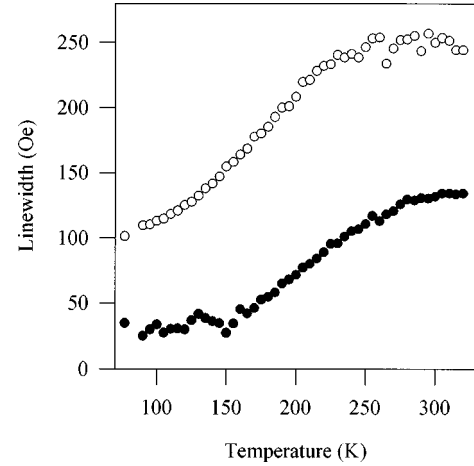


FIG. 2. FMR linewidths of single crystal (●) and polycrystalline (○) manganese ferrites ( $\text{Mn}_{1.0}\text{Fe}_{2.0}\text{O}_4$ ).

where  $H$  is the static field,  $\Delta H$  is the FMR linewidth, and  $H_0$  is the resonance field. Gaussian units will be used throughout this work.

The variation of the FMR linewidth with temperature is presented in Fig. 2. The maximum experimental error estimated is about 5%.

Manganese ferrite is characterized by its high saturation magnetization (7000 G at 0 K). The use of our cylindrical cavity working in  $\text{TE}_{111}$  mode, involves resonance fields of 3000 Oe. This field assures the saturation of the sample as seen in Fig. 3; however, the permanence of uniform precession mode inside the SWM is not satisfied. If we substitute field values in expression  $\gamma(H_i + 2\pi M_S)$ , the operational frequency (8.9 GHz), although is out of the SWM, is inside the magnetostatic mode spectrum.

The FMR line shape on examination shows a symmetrical peak. There is no reason for more peaks to appear because the sample is small enough and it is placed at a point in the cavity where the rf magnetic field is sufficiently homogeneous. Since the permanence of the uniform precession mode inside the SWM is not satisfied, it should be necessary to use Eqs. (5), (7), and (10) to obtain the different two-magnon contributions to the linewidth. If we use the data of the poly-

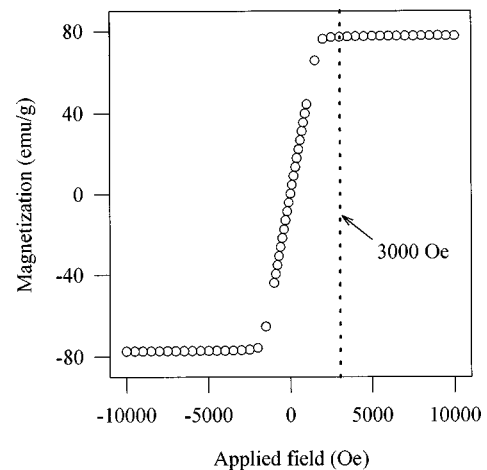


FIG. 3. Hysteresis loop for polycrystalline manganese ferrite ( $\text{Mn}_{1.0}\text{Fe}_{2.0}\text{O}_4$ ) at room temperature.

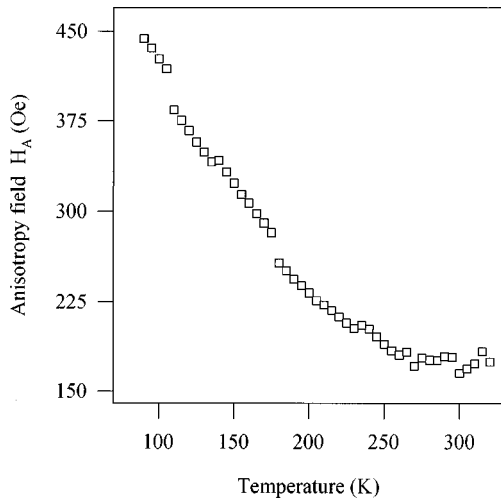


FIG. 4. Anisotropy field for polycrystalline manganese ferrite ( $\text{Mn}_{1.0}\text{Fe}_{2.0}\text{O}_4$ ).

crystalline sample ( $4\pi M_S = 6500$  G,  $\omega/\gamma = 3150$  Oe, and  $H_A = 465$  Oe at 77 K) the contributions to the linewidth from the superficial, porosity, and anisotropy mechanism are

$$\Delta H_{\text{sup}} \approx 1300 G(\theta_u) \text{ Oe}; \quad \Delta H_{\text{por}} \approx 2600 G(\theta_u) \text{ Oe};$$

$$\Delta H_A \approx 200 G(\theta_u) \text{ Oe},$$

respectively.

It can be observed that the anisotropy linewidth is 5% of the superficial and porosity contributions together, so it can be neglected, without performing an error larger than the experimental one. This assumption is consistent with the theory for isotropic or with relatively small levels of magnetocrystalline anisotropic materials. Anisotropy fields observed for our samples are presented in Fig. 4.

In order to obtain the superficial contribution to the linewidth it is necessary to use the expression given by Eq. (5). Magnetization as a function of temperature has been measured using a vibrating-sample magnetometer and fitting the experimental results by means of the  $T^{3/2}$  law. Magnetic moment per molecule obtained is  $4.78\mu_B$  ( $\mu_B$  is the Bohr magneton) for polycrystalline sample. The fitting attained is presented in Fig. 5.

The sample radius is 0.4 mm; the resonance field value ( $H_0 = \omega/\gamma$ ) has been obtained from the operational frequency (8.9 GHz) and using  $g$  values given in the literature [ $g(77) = 2.019$ ;  $g(300) = 2.004$ ].<sup>38</sup> The only unknown parameters are the pit radius ( $R$ ) and the  $G(\theta_u)$  function. They have been obtained by means of an iterative program which presents the most suitable parameters for each set of experimental data. The fitting of the experimental data for the single crystal can be observed in Fig. 6.

The experimental results can be fitted by means of superficial and eddy current contributions. The sum of these two mechanisms is what we have called the theoretical result. The difference between experimental data and the theoretical result gives us a notion about the committed error, which we call the residual linewidth.

With this fitting, the superficial contribution for  $R$ , the pit radius, is 0.05 mm which agrees very well with the expected size (is on the same order of magnitude as the polishing

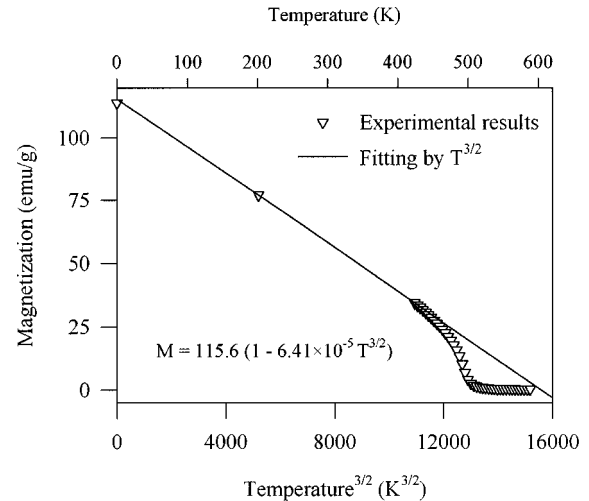


FIG. 5. Magnetization fitting by  $T^{3/2}$  law for polycrystalline manganese ferrite ( $\text{Mn}_{1.0}\text{Fe}_{2.0}\text{O}_4$ ).

material used) and for  $G(\theta_u) \approx 2 \times 10^{-2}$ . For the eddy current contribution we obtain a value of 0.06 eV for the activation energy and  $85 \Omega \text{ cm}^{-1} \text{ K}$  for the  $C$  constant of Eq. (12). This activation energy is on the order of the magnitude of the electronic hopping between  $\text{Fe}^{2+}$  and  $\text{Fe}^{3+}$ .<sup>39-41</sup> The residual linewidth is lower than 5 Oe which shows the correctness of the fitting.

In the polycrystalline sample the porosity contribution should also be included. Since the superficial mechanism only depends on the geometry of the sample and the composition, it is reasonable to think that for single and polycrystalline samples, with the same composition and similar sizes, the contribution will be the same for both. To analyze porosity contribution it is necessary to assume that the parameter  $G(\theta_u)$  is the same as the one obtained from superficial contribution in the case of single crystal. Adopting this procedure, the fitting of the linewidth for the polycrystalline manganese ferrite is presented in Fig. 7. The fitting parameters are 3% for porosity and 0.04 eV for activation energy and  $54 \Omega \text{ cm}^{-1} \text{ K}$  for the  $C$  constant of Eq. (12). The residual linewidth is lower than 7 Oe.

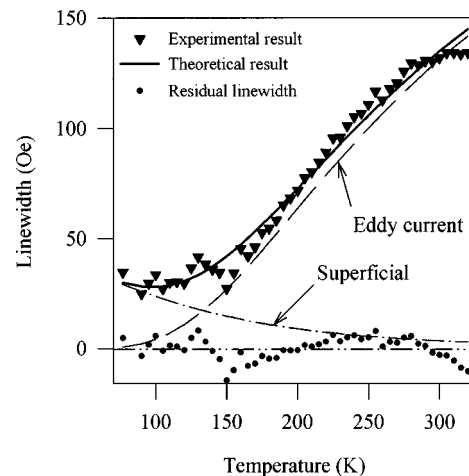


FIG. 6. Fitting of the linewidth for single-crystal manganese ferrite ( $\text{Mn}_{1.0}\text{Fe}_{2.0}\text{O}_4$ ). The theoretical result is the sum of all contributions present while the difference between experimental and theoretical results is called the residual linewidth.

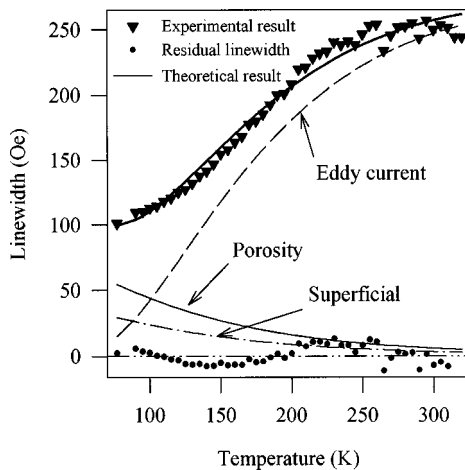


FIG. 7. Fitting of the linewidth for polycrystalline manganese ferrite ( $\text{Mn}_{1.0}\text{Fe}_{2.0}\text{O}_4$ ). The theoretical result is the sum of all contributions present while the difference between experimental and theoretical results is called the residual linewidth.

#### IV. CONCLUSIONS

It can be concluded that in ferrimagnetic resonance experiments with single and polycrystalline ferrites, working with fields only slightly larger than the value  $4\pi N_z M$  required to saturate the sample, the two-magnon theory developed in ferromagnetic relaxation is not valid. For such cases, an experimental procedure has been developed in order to obtain the superficial and porosity contributions to the linewidth. Compared with these linewidths, the anisotropy contribution that appears in polycrystalline samples is neglected.

This approach utilizes a function  $G(\theta_u)$  temperature independent which can be obtained by means of experimental results in single-crystal samples. The value of this function is applicable to porosity and anisotropy contributions.

In single-crystal manganese ferrites, superficial and eddy-current contributions to the linewidth are present. In polycrystalline manganese ferrites, superficial contribution is the same as the correspondent contribution in single crystals, while porosity and eddy-current contributions also appear. With our two-magnon linewidth approach, the parameters needed for the fitting have been obtained, getting errors lower than 4%. The presence of the eddy-current contributions indicates the existence of conduction electrons; the values of the activation energies fitted (0.06 and 0.04 eV for single and polycrystalline samples, respectively) implies the existence of  $\text{Fe}^{2+}$  cations in  $\text{Mn}_{1.0}\text{Fe}_{2.0}\text{O}_4$ ,<sup>39–41</sup> since the activation energies necessary for the other possible hopping mechanism  $\text{Fe}^{3+} + \text{Mn}^{2+} \leftrightarrow \text{Fe}^{2+} + \text{Mn}^{3+}$  are of the order of magnitude  $\sim 0.3$  eV.<sup>39</sup> With these parameters the values obtained for the conductivity are at 300 K  $\sigma(300) \approx 0.04 \Omega \text{ cm}^{-1}$  for the polycrystal and  $\sigma(300) \approx 0.03 \Omega \text{ cm}^{-1}$  for the single crystal.

#### ACKNOWLEDGMENT

This work was partially supported by the Consejería de Fomento de la Junta de Castilla y León under Project No. SA0197, and by project MAT98-0416-C03-03. A.G.F. thanks Ministerio de Educación y Cultura for having been awarded a grant of the “Subprograma General de Perfeccionamiento de Doctores en el Extranjero.”

\*Electronic address: anagf@gugu.usal.es

- <sup>1</sup>J. P. Chen, C. M. Sorensen, K. J. Klabunde, G. C. Hadjipanayis, E. Devlin, and A. Kostikas, *Phys. Rev. B* **54**, 9288 (1996).
- <sup>2</sup>Z. X. Tang, C. M. Sorensen, K. J. Klabunde, and G. C. Hadjipanayis, *J. Appl. Phys.* **69**, 5279 (1991).
- <sup>3</sup>V. A. M. Brabers, *Phys. Rev. Lett.* **68**, 3113 (1992).
- <sup>4</sup>Z. X. Tang, C. M. Sorensen, K. J. Klabunde, and G. C. Hadjipanayis, *Phys. Rev. Lett.* **67**, 3602 (1991).
- <sup>5</sup>P. J. Van der Zaag, V. A. M. Brabers, M. T. Johnson, A. Noordermeer, and P. F. Bengers, *Phys. Rev. B* **51**, 12 009 (1995).
- <sup>6</sup>A. R. Corradi, L. Benzoni, N. Burriesci, C. A. Nannetti, M. P. Pettera, and S. Pizzini, *J. Phys. Colloq.* **4** (38), C1-291 (1977).
- <sup>7</sup>J. B. Sokoloff, *J. Appl. Phys.* **66**, 3187 (1989).
- <sup>8</sup>J. B. Sokoloff, *J. Appl. Phys.* **79**, 4564 (1996).
- <sup>9</sup>R. Mahendiran, S. K. Tiwary, A. K. Raychaudhuri, T. V. Ramakrishnan, R. Mahesh, N. Rangavittal, and C. N. R. Rao, *Phys. Rev. B* **53**, 3348 (1996).
- <sup>10</sup>Jun Zang, A. R. Bishop, and H. Röder, *Phys. Rev. B* **53**, R8840 (1996).
- <sup>11</sup>T. A. Tyson, J. Mustre de Leon, S. D. Conradon, A. R. Bishop, J. Neumeier, H. Röder, and Jun Zang, *Phys. Rev. B* **53**, 13 985 (1996).
- <sup>12</sup>G. J. Snyder, R. Hiskes, S. DiCarolis, M. R. Beasley, and T. H. Geballe, *Phys. Rev. B* **53**, 14 434 (1996).
- <sup>13</sup>S. E. Lofland, P. H. Kim, P. Dahiroc, S. M. Bhagat, S. D. Tyagi, C. Kwon, R. Shreekal, R. Ramesh, and T. Venkatesan, *J. Phys.: Condens. Matter* **9**, 6697 (1997).

- <sup>14</sup>S. E. Loafand, S. M. Bhagat, H. L. Ju, C. G. Xiong, T. Venkatesan, and R. L. Greene, *Phys. Rev. B* **52**, 15 058 (1995).
- <sup>15</sup>M. Dominguez, S. E. Loafand, S. M. Bhagat, A. K. Raychaudhuri, H. L. Ju, T. Venkatesan, and R. L. Greene, *Solid State Commun.* **97**, 193 (1996).
- <sup>16</sup>S. B. Oseroff, M. Torikachvili, J. Singley, S. Ali, S. W. Cheong, and S. Schultz, *Phys. Rev. B* **53**, 6521 (1996).
- <sup>17</sup>L. Torres, M. Zazo, J. Iñiguez, and M. Quintillán, *Appl. Phys. A: Solids Surf.* **55**, 154 (1992).
- <sup>18</sup>L. Torres, M. Zazo, J. Iñiguez, C. de Francisco, and J. M. Muñoz, *IEEE Trans. Magn.* **29**, 3434 (1993).
- <sup>19</sup>L. Torres, M. Zazo, J. Iñiguez, C. de Francisco, and J. M. Muñoz, *Appl. Phys. A: Mater. Sci. Process.* **60**, 303 (1995).
- <sup>20</sup>A. G. Flores, L. Torres, M. Zazo, V. Raposo, and J. Iñiguez, *Appl. Phys. Lett.* **67**, 427 (1995).
- <sup>21</sup>L. Torres, A. G. Flores, M. Zazo, A. R. Ferreira, C. S. Furtado, J. M. Perdigao, C. de Francisco, and J. Rivas, *Phys. Status Solidi A* **153**, 213 (1996).
- <sup>22</sup>L. Torres, M. Zazo, A. G. Flores, V. Raposo, and J. Iñiguez, *J. Appl. Phys.* **79**, 5422 (1996).
- <sup>23</sup>L. Torres, M. Zazo, J. Iñiguez, C. de Francisco, J. Muñoz, and P. Hernandez, *J. Appl. Phys.* **79**, 5436 (1996).
- <sup>24</sup>A. G. Flores, L. Torres, V. Raposo, L. López-Díaz, M. Zazo, and J. Iñiguez, *Phys. Status Solidi A* **171**, 549 (1999).
- <sup>25</sup>M. Sparks, R. Loudon, and C. Kittel, *Phys. Rev.* **122**, 791 (1961).
- <sup>26</sup>E. Schlömann, *J. Phys. Chem. Solids* **6**, 242 (1958); **6**, 257 (1958).

- <sup>27</sup>M. Sparks, *Ferromagnetic Relaxation Theory* (McGraw-Hill, New York, 1965).
- <sup>28</sup>C. E. Patton, in *Magnetic Oxides*, edited by D. J. Craik (Wiley, London, 1975), Chap. 10.
- <sup>29</sup>M. J. Hurben, D. R. Franklin, and C. E. Patton, *J. Appl. Phys.* **81**, 7458 (1997).
- <sup>30</sup>M. J. Hurben and C. E. Patton, *J. Appl. Phys.* **83**, 4344 (1998).
- <sup>31</sup>L. R. Walker, *J. Appl. Phys.* **29**, 318 (1958).
- <sup>32</sup>R. L. White and I. H. Solt Jr., *Phys. Rev.* **104**, 56 (1956).
- <sup>33</sup>J. F. Dillon Jr., *Phys. Rev.* **112**, 59 (1958).
- <sup>34</sup>V. B. Anfinogenov, L. A. Mitlina, A. F. Popkov, A. A. Sidorov, V. G. Sokorin, and V. V. Tikhonov, *Sov. Phys. Solid State* **30**, 1172 (1989).
- <sup>35</sup>P. Röschmann, *IEEE Trans. Magn.* **Mag-11**, 1247 (1975).
- <sup>36</sup>Kee Tae Han, *Phys. Status Solidi A* **155**, 215 (1996).
- <sup>37</sup>C. J. Brower and C. E. Patton, *J. Appl. Phys.* **53**, 2104 (1982).
- <sup>38</sup>J. Smit and H. P. J. Wijn, *Ferritas* (Biblioteca Técnica Philips, Paraninfo, 1965).
- <sup>39</sup>F. K. Lotgerin, *J. Phys. Chem. Solids* **25**, 95 (1964).
- <sup>40</sup>V. A. M. Brabers and A. A. Scheerder, *IEEE Trans. Magn.* **24**, 1907 (1988).
- <sup>41</sup>Z. Simsa and V. A. M. Brabers, *IEEE Trans. Magn.* **24**, 1841 (1988).